

Influence of the pseudopotential on the properties of liquid rubidium at 315 K

J. M. González Miranda

Departamento de Termología, Facultad de Física, Universidad de Barcelona, Diagonal 645, 08028 Barcelona, Spain

(Received 17 September 1986)

The influence of the pseudopotential on both the structure and the self-diffusion of liquid rubidium at the melting point has been investigated by means of molecular-dynamics calculations. The model potential considered has been computed from the pseudopotential of Ashcroft, the dielectric function of Geldart and Vosko, and a Born-Mayer term. Four different values for the core radius which enters as input in the pseudopotential have been considered. In this way we have been able to observe and interpret the effect of this contribution on the properties of the liquid.

I. INTRODUCTION

The effective ion-ion potential in simple metals can be obtained as a screened Coulomb interaction that includes the Coulomb repulsion between bare ion cores as well as conduction-electron screening computed by means of pseudopotentials and dielectric functions.¹ Moreover, some authors add a core-overlap interaction which takes account of the exchange forces which occur when wave functions of adjacent cores overlap.² These pair potentials are being widely used in liquid-state physics as input for theoretical models^{3,4} or computer experiments.^{5,6} They are also used as references to compare empirical pair potentials obtained from measured structure factors by inversion of approximate theories of the structure of liquids.⁷

For the pseudopotential, which plays a fundamental role in the calculation of the screening potential, one can find in the literature two possibilities: (i) nonlocal pseudopotentials which are constructed from fundamental atomic properties such as the atomic number, the atomic mass, and the wave functions and eigenenergies of core electrons for the isolated ion, and (ii) local pseudopotentials, which contain drastic idealizations of the ion-electron interactions and depend on adjustable parameters. While the former are difficult to compute, the latter are quite simple and their use has become very popular among the people working on liquid-state physics. Particularly, Ashcroft⁸ and Heine and Abarenkov's⁹ potentials, which depend only on one and two parameters, respectively, are being widely and successfully used in studies of simple liquids, mainly those of the alkali metals.³⁻⁶

The parameters of the local potentials are usually fitted to obtain good agreement with experiment for some properties. Elastic constants,¹⁰ the shape of the Fermi surface,¹¹ or the correct equilibrium density at $T=0$ K,⁴ for the corresponding crystalline metal are the most commonly used properties for solids. For liquids one uses the electrical resistivity¹² or the self-diffusion constant.¹³ A look at the literature on the physics of liquids will show that the values of the parameters currently used for this kind of pseudopotential vary over a wide range, as they are provided by different authors. Therefore it is of interest

to study the influence of the parameters employed in the pseudopotential on the properties of the liquid.

In this spirit we will present here a molecular-dynamics (MD) study of liquid Rb near the melting point where the influence of the pseudopotential of Ashcroft on the structure and self-diffusion of the liquid is observed and discussed. All the pair potential functions considered have been computed from the pseudopotential of Ashcroft, which is determined by the empty-core ionic radius, a single adjustable parameter for which different values have been reported by several authors.^{4,8,11,13} Then, we consider various pseudopotentials for Rb computed from the model of Ashcroft but with different values of R_A as input. In this way we have been able to observe the influence of the pseudopotential on the pair potential and then on the several properties of the liquid that we compute by means of the MD method.

Moreover, some interesting conclusions are drawn from the comparison of the results reported here on the sensitivity of the properties of Rb to the pseudopotential with a recent study by González Miranda and Torra¹⁴ on the sensitivity of the properties of Na to the dielectric function. Although different metals are being considered, both are alkali metals and in both cases the pair potentials have been computed from Ashcroft's empty-core model potential. Then, as we will consider only relative values for the quantities that we are going to compare, we expect that we can draw some meaningful conclusions from comparison of our results with those of Ref. 14.

II. EFFECTIVE PAIR POTENTIALS

The theoretical model for the effective pair potential in a liquid metal has been recently reviewed by Ashcroft and Stroud.¹ Basically it is computed from

$$\Phi(r) = \frac{Z^2 e^2}{r} - \frac{1}{2\pi^2} \int k^2 \frac{\sin(kr)}{kr} F(k) dk + A e^{-\alpha r}, \quad (1)$$

the first term being the Coulomb repulsion, the second the screening potential, and the third the overlap interaction.² In this expression Z is the valence of the ion, and A and α characteristic parameters of the substance. The shape of the function $F(k)$ is determined by the pseudopotential

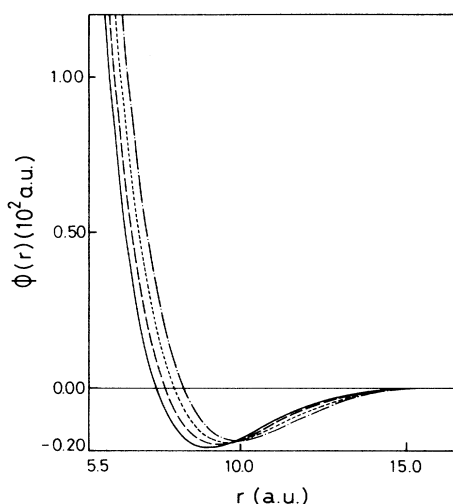


FIG. 1. Effective pair potentials for liquid Rb at 315 K: solid line, Rb(1); dashed line, Rb(2); dotted line, Rb(3); and dotted-dashed line, Rb(4). Atomic units (a.u.) are used for energy and length.

and the dielectric function.¹

The effective pair potentials considered here have been computed from the pseudopotential of Ashcroft⁸ and the dielectric function of Geldart and Vosko.¹⁵ This simple model potential has proved to be particularly good for liquid Na (Ref. 14) and has been used recently by Berezhkovsky *et al.*⁵ to study transport properties in liquid Na and K, and by Fukase *et al.*⁶ to compute a suitable model potential for metal-salt ionic solutions. The values for the input parameters used here are $Z = 1$, $A = 61.3$ a.u., and $\alpha = 1.53$ a.u. Moreover, the values for R_A have been taken from various authors in the literature as summarized in Table I.

We have computed four different potential functions for Rb. These will be denoted by Rb(1), Rb(2), Rb(3), and Rb(4) throughout the paper. As shown in Table I, the value of R_A increases from Rb(1) to Rb(4). These pair potentials are displayed in Fig. 1. They show a similar shape with a relatively soft wall, a well about -0.15×10^{-2} a.u. deep, and then an evolution to zero with a node near 16.7 a.u. The long-range behavior, not

TABLE I. Values for the parameter R_A used as input in the various pair potentials considered. Moreover, the position of the first zero of the pair potential denoted by σ has been included together with the characteristic interparticle separation $r_s = [3\pi/(4\Omega)]^{1/3}$, Ω being the specific volume per particle of the liquid.

Potential	R_A (a.u.)	σ (a.u.)	σ/r_s
Rb(1)	2.39 ^a	7.18	1.33
Rb(2)	2.49 ^b	7.47	1.38
Rb(3)	2.61 ^c	7.98	1.48
Rb(4)	2.72 ^d	8.27	1.53

^aReference 13.

^bReference 4.

^cReference 11.

^dReference 8.

shown in the figure, has oscillations of decreasing amplitude. These are always smaller than 0.01 of the depth of the well. The main effect of increasing the empty-core radius is a displacement of each pair potential as a whole to the right. Moreover, a small decrease of the depth of the well is also observed. The first trend is related to the increase of the core radius, which means that we consider larger ions. This is shown in Table I where the value of σ , the position of the first node of the several potentials, has been inserted. Comparison of σ and R_A shows that a relation of the type $\sigma = 3R_A$ is verified within a few per cent. The second trend is characteristic of the dielectric function and other dielectric functions will give a different behavior.¹⁶

III. MOLECULAR-DYNAMICS CALCULATIONS

A. Computational details

For each of the above pair potentials we have computed a MD run. In these calculations the potentials were truncated at the third node, thus neglecting very small contributions to the pair potential. Our calculations have been devised to simulate a thermodynamic state close to the melting point ($T = 315$ K and $\rho = 1.463$ g cm⁻³). We have considered 686 particles enclosed in a cubic box with an edge $L = 76.6$ a.u. The Newtonian equations of motion have been integrated by means of a predictor-corrector algorithm with a time step $\tau = 1.44 \times 10^{-14}$ s. This gives a satisfactory conservation of energy. The time evolution of the system was followed for 1600 time steps after reaching equilibrium. The statistical error of the quantities so obtained are small enough to ensure that our results are reliable.¹⁷

B. Structure

In order to study the structure of the liquids, we have computed the pair correlation function,

$$g(r) = \frac{L^3}{N} \frac{\langle d\bar{n}(r) \rangle}{4\pi r^2 dr}, \quad (2)$$

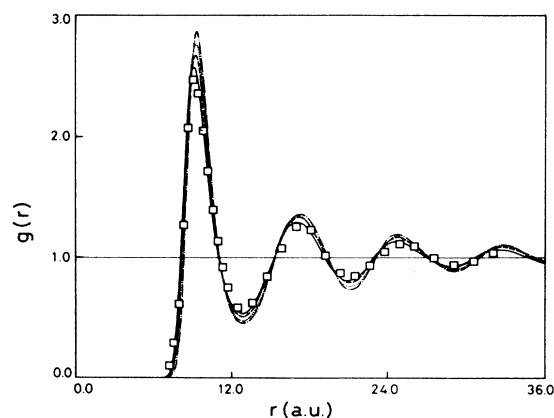


FIG. 2. Pair distribution functions for liquid Rb at 315 K computed from the pair potentials of Fig. 1. The curves are as in this figure. Moreover the experimental results by Waseda (Ref. 19), denoted by squares, have been inserted.

TABLE II. Positions of the first four peaks of $g(r)$, (r_i , $i=1,2,3,4$) for the pair potentials considered. The values of r_i are given both in a.u. and in units of σ (figures in parentheses).

Potential	r_1	r_2	r_3	r_4
Rb(1)	9.1(1.27)	17.1(2.37)	24.7(3.44)	32.5(4.53)
Rb(2)	9.2(1.23)	17.3(2.31)	24.9(3.33)	32.9(4.40)
Rb(3)	9.3(1.17)	24.9(2.18)	24.9(3.12)	32.9(4.12)
Rb(4)	9.4(1.14)	17.5(2.12)	24.9(3.01)	33.0(3.99)

where $d\bar{n}(r)$ is the mean number of particles at a distance between r and $r+dr$ away from a given particle and the angular brackets denote a time average. The results obtained are displayed in Fig. 2. They show a marked variation with changes in the pseudopotential, which affects both the heights and positions of the peaks and valleys. As the core radius increases the positions of the peaks and valleys undergo small but observable displacements to the right, the first peak increases noticeably, and the damping of the long-range oscillations becomes smaller. Moreover, in Table II we have displayed the positions of the peaks of $g(r)$. These are given both in a.u. and in units of σ (defined in Sec. II), in this second case the peaks appear shifted towards smaller values of r .

This evolution of $g(r)$ with core radius can be understood if one takes into account that the effect of an increase of the density in classical liquids is basically to enhance the peaks and valleys of $g(r)$ and to shift the pair correlation functions towards smaller values of r .¹⁸ These trends are qualitatively similar to those observed here with increasing R_A , when the positions are measured in units of σ . On the other hand, as shown in Table I, the main effect of R_A on the pair potential is to increase σ and thus the ratio σ/r_s , r_s being the radius of the sphere whose volume equals the specific volume of the liquid. Therefore the reduced density of the liquid $n^*=n\sigma^3$, n being the number density, increases with increasing core radius giving rise to an evolution of $g(r)$ analogous to that due to increasing density.

Moreover, we can say something further about the sensitivity of the structure to the pair potentials considered. We have obtained here an increase of about 13% in the height of the peaks of $g(r)$ with an increase of 14% in the value of the core radius when Rb(1) and Rb(4) are compared. Similar relative results hold for other couples of pair potentials. These are much greater than those reported by González Miranda and Torra¹⁴ for the dielectric function: 5% for the pair of dielectric functions which gave the more different $g(r)$. Moreover, while the changes in dielectric function do not produce observable variations in the positions of the peaks and valleys, those due to the change of pseudopotential are observable (although they are an order of magnitude smaller than those of R_A). Then the contribution which primarily determines the structure of the liquid is the pseudopotential, while the dielectric function plays only a secondary role.

Our results for $g(r)$ are also compared with experiment in Fig. 2. There the neutron diffraction determination by Waseda¹⁹ has been inserted. Our functions are more structured, showing in all cases higher peaks and lower valleys. Moreover they locate satisfactorily the positions

of maxima and minima, and only a small shift to the left is obtained for the secondary peaks and valleys. The overall good agreement obtained, which is better for Rb(1), indicates that the model potential considered is a realistic approximation for real Rb.

C. Self-diffusion

In order to study single-particle motion we have computed the normalized velocity correlation function

$$\psi_N(t) = \frac{\left\langle \sum_{i=1}^N (\mathbf{v}_i(0) \cdot \mathbf{v}_i(t)) \right\rangle}{\left\langle \sum_{i=1}^N v_i^2(0) \right\rangle} \quad (3)$$

and the mean-square displacement

$$r^2(t) = \frac{1}{N} \left\langle \sum_{i=1}^N |\mathbf{r}_i(t) - \mathbf{r}_i(0)|^2 \right\rangle. \quad (4)$$

Both functions allow us to obtain the self-diffusion constant in a direct way, and the former together with its density spectrum is particularly informative on the details of the diffusive behavior of the liquid. Our results are displayed in Figs. 3–5. The unit of time used there equals 1.033×10^{-15} s. This has been chosen to produce

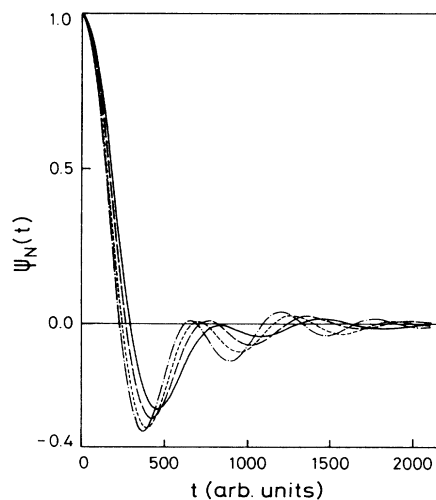


FIG. 3. Normalized velocity correlation functions for liquid Rb at 315 K for potentials Rb(1) to Rb(4). The curves are as in Figure 1. The unit of time is 1.033×10^{-15} s.

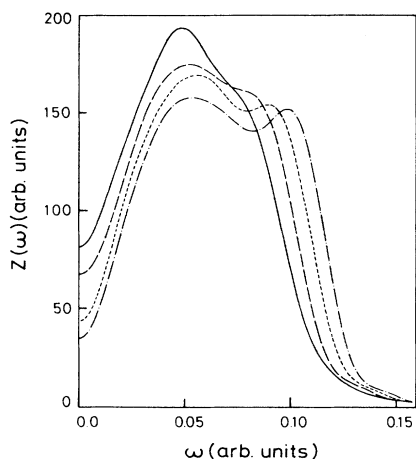


FIG. 4. Spectral densities of the velocity correlation functions of Fig. 3. The unit for both $z(\omega)$ and ω is $9.68 \times 10^{14} \text{ s}^{-1}$.

numerical values for times and frequencies of a reasonable size. Therefore the units for these quantities will be denoted arb. units, instead of a.u. used for atomic units.

The functions $\psi_N(t)$ obtained show a rapid initial decay followed by the oscillatory evolution to zero characteristic of liquid metals. As R_A increases the oscillations become more damped and the positions of maxima and minima move towards larger times.

The behavior of $\psi_N(t)$ for classical liquids has been interpreted recently by Balucani *et al.*^{20,21} in terms of the time evolution of the momentum transfer from a central particle to its surroundings. Basically, the rapid initial decay in $\psi_N(t)$ means that the test particle loses momentum by pulling in the first and second shells of its neighbors. The minimum and the positive slope are due to a subsequent spread of momentum from these neighbor shells which partly returns to the test particle. The long-range oscillations are due to the relatively important relation between cohesive and repulsive forces in metals. This means that an atom is coupled to the first shells of its neighbors for a long time. Although, to our knowledge, no detailed studies of the dependence with density for liquid metals have been performed, Balucani *et al.*²⁰ have studied the process at two different densities for a Lennard-Jones system showing that at low densities the transfer of momentum becomes slow and if the density is small enough, the test particle loses only forward momentum and is not reversed. Taking this result into account, we can understand the trends observed in $\psi_N(t)$ in terms of these ideas and the observation in the preceding section on the reduced density of the liquid. If we accept that a low density gives rise to a slow transfer of momentum and a decrease of the quantity transferred at all times, then the trends observed here are clearly understood. This indicates that also for single-particle motion the changes performed in the pair potential give rise to increased-density-like trends in $\psi_N(t)$ associated with the change in reduced density of the system.

A complementary view can be obtained from the results for the spectral density of the velocity correlation function, $z(\omega)$, displayed in Fig. 4. The functions have a

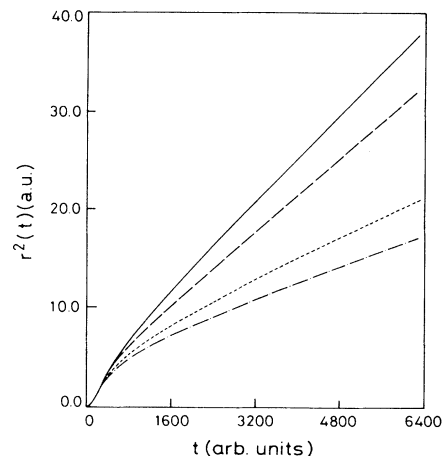


FIG. 5. Mean-square displacement as a function of time for liquid Rb at 315 K. The curves are as in Fig. 1.

nonzero value at $\omega=0$, increase to a maximum at about $\omega=0.45 \times 10^{-2}$ arb. units and then evolve to zero showing a shoulder near $\omega=0.45 \times 10^{-2}$ arb. units. The increase in core radius gives rise to a decrease in the zero-frequency value and enhances the maximum and the shoulder. This last area becomes practically a secondary maximum for Rb(3) and Rb(4). The position of the main peak is practically unaffected and that of the shoulder is shifted to the right.

In a recent paper Endo *et al.*²² have reported MD calculations for the spectrum of $\psi_N(t)$ for inverse power potentials at different densities. The evolution with increasing density reported for the density region around that studied here was qualitatively similar to that observed above for increasing core radius. This clearly reinforces our interpretation of the action of the pseudopotential as a density-like effect.

In order to compare with experiment, we have computed the self-diffusion constant of the liquids, both from the time integral of $\psi_N(t)$ (Fig. 3) and from the slope of the long-time behavior of $r^2(t)$ (Fig. 5). The results obtained appear in Table III. There it is seen that both sets of values are consistent. This indicates the accuracy of the values obtained. A single trend is observed: the increase in core radius gives rise to a decrease in the value of the self-diffusion constant. All our values are smaller than the experimental one of $2.62 \times 10^{-5} \text{ cm}^2 \text{ s}^{-1}$ reported by Norden and Lodding.²³ As the overall agreement is good, being also better for Rb(1), our confidence in the reliability of the simple pair potential model considered to represent real Rb is reinforced.

The self-diffusion constant is also found to be very sensitive to the change performed to the pseudopotential. We observe a decrease of 57% in the self-diffusion constant when Rb(1) and Rb(4) are compared, and relative similar results for the other couples of pair potentials. On the other hand, the largest difference between a couple of values of D found by González Miranda and Torra¹⁴ was about 26%. Then, for the diffusive behavior the pseudopotential plays a role which, although more important than that of the dielectric function, is comparable to it.

TABLE III. Values for the self-diffusion constant computed from the various pair potentials considered. D_ψ has been obtained from $\psi_N(t)$ and D_r from $r^2(t)$. The estimated errors of our calculations are about 3%. The experimental value reported by Norden and Lodding (Ref. 23) is $2.62 \cdot 10^{-5} \text{ cm}^2 \text{ s}^{-1}$.

Potential	D_ψ ($10^{-5} \text{ cm}^2 \text{ s}^{-1}$)	D_r ($10^{-5} \text{ cm}^2 \text{ s}^{-1}$)
Rb(1)	2.46	2.42
Rb(2)	2.06	2.14
Rb(3)	1.32	1.26
Rb(4)	1.07	0.98

IV. SUMMARY

The qualitative and quantitative influence of the pseudopotential on the properties of liquid Rb near the melting point have been investigated by means of a MD simulation. Comparison with experiment has proved that the pair potential model used is reliable, and then the following points are meaningful:

(i) The height of the peaks and the depth of the valleys of the pair distribution function undergo an increase with R_A of the same order of magnitude as R_A . The positions of peaks and valleys shift to the right by an amount which is about an order of magnitude smaller.

(ii) The self-diffusion constant decreases with R_A by an amount about three times greater than the change performed. These changes and those of point (i) are not negligible and care should be taken in choosing values for R_A for any specific application. A similar observation

will surely hold for other local pseudopotentials.

(iii) The trends of structure and self-diffusion with core radius are qualitatively analogous to those associated with the change of density of the liquid. This has been interpreted in terms of the ratio σ/r_s , which informs us of the relation between the size of the particles considered and the volume available per particle.

(iv) Comparison with previous work indicates that the structure of the liquid is mainly determined by the pseudopotential, but its relative influence in self-diffusion is roughly of the same order of magnitude as that of the dielectric function.

(v) In the comparison with experiment the pseudopotential parameter $R_A = 2.39$ a.u. is favored both for structure and transport. It should be noted that this value is consistent with others proposed in the literature to obtain good agreement with experiment for different properties of solid Rb. It is very close to $R_A = 2.40$ a.u., reported by Price, Singwi, and Tosi²⁴ in a study of phonon dispersion curves, and by Hartmann²⁵ in calculations of the latent heat of melting. It is also close to $R_A = 2.43$ a.u., proposed by Shyu, Singwi, and Tosi,²⁶ in a study of force constants and velocity of sound.

ACKNOWLEDGMENT

The calculations reported in this paper have been performed with the computer IBM 4340 of the Centro de Calculo de la Universidad de Barcelona.

¹N. W. Ashcroft and D. Stroud, *Solid State Phys.* **33**, 1 (1978).

²R. Benedek, *Phys. Rev. B* **15**, 2902 (1977); T. Lee, J. Bishop, W. van der Lugt, and W. F. van Gunsteren, *Physica B* **93**, 59 (1978).

³A. M. Bratkovsky and V. G. Vaks, *J. Phys. F* **13**, 2707 (1983).

⁴G. Kahl and J. Hafer, *Z. Phys. B* **58**, 283 (1985).

⁵L. M. Berezhkovsky, A. N. Drozdov, V. Yu Zitserman, A. N. Lagar'kov, and S. A. Tiger, *J. Phys. F* **14**, 2315 (1984).

⁶S. Fukase, S. Naito, R. Takagi, and K. Kawamura, *J. Phys. F* **15**, 1867 (1985).

⁷W. G. Madden and S. A. Rice, *J. Chem. Phys.* **72**, 4208 (1980); I. Yokojama and S. Ono, *Phys. Chem. Liq.* **14**, 83 (1984).

⁸N. W. Ashcroft, *Phys. Lett.* **23**, 48 (1966).

⁹V. Heine and I. Abarenkov, *Philos. Mag.* **9**, 451 (1964).

¹⁰P. S. Ho, *Phys. Rev.* **169**, 523 (1968).

¹¹M. L. Cohen and V. Heine, *Solid State Phys.* **24**, 37 (1980).

¹²N. W. Ashcroft and D. C. Langreth, *Phys. Rev.* **159**, 500 (1967).

¹³J. M. González Miranda, *Physics B* (to be published).

¹⁴J. M. González Miranda and V. Torra, *J. Phys. F* **13**, 282 (1983).

¹⁵D. J. W. Geldart and S. H. Vosko, *Can. J. Phys.* **44**, 2137

(1966).

¹⁶J. M. González Miranda and V. Torra, *An. Fis.* **78**, 172 (1982).

¹⁷R. Zwanzig and N. K. Ailawadi, *Phys. Rev.* **182**, 280 (1969).

¹⁸C. J. Pings, in *Physics of Simple Liquids* (North-Holland, Amsterdam, 1968) Chap. 10.; M. Tanaka, *J. Phys. F* **10**, 2581 (1980).

¹⁹Y. Waseda, *The Structure of Non-Crystalline Materials* (McGraw-Hill, New York, 1981).

²⁰U. Balucani, R. Vallauri, and C. S. Murthy, *Phys. Lett. A* **84**, 133 (1981).

²¹U. Balucani, R. Villary, and C. S. Murthy, *J. Chem. Phys.* **77**, 2233 (1982).

²²H. Endo, Y. Endo, and N. Ogita, *J. Chem. Phys.* **77**, 5184 (1982).

²³A. Norden and A. Lodding, *Z. Naturforschung.* **22a**, 215 (1967).

²⁴D. L. Price, K. S. Singwi, and M. P. Tosi, *Phys. Rev. B* **2**, 2983 (1970).

²⁵W. M. Hartman, *Phys. Rev. Lett.* **26**, 1640 (1971).

²⁶Wei-Mei Shyu, K. S. Singwi, and M. P. Tosi, *Phys. Rev. B* **3**, 237 (1971).